# Supplementary Information

Mechanistic classification and benchmarking of polyolefin depolymerization over silica-alumina-based catalysts

Wei-Tse Lee[1], Antoine van Muyden[1], Felix D. Bobbink[1], Mounir D. Mensi[1], Jed R. Carullo[1], Paul J. Dyson[1,*]

[1]Institute of Chemical Sciences and Engineering, École Polytechnique Fédérale de Lausanne (EPFL), Lausanne, Switzerland.
[*]Corresponding author: Paul J. Dyson (paul.dyson@epfl.ch)

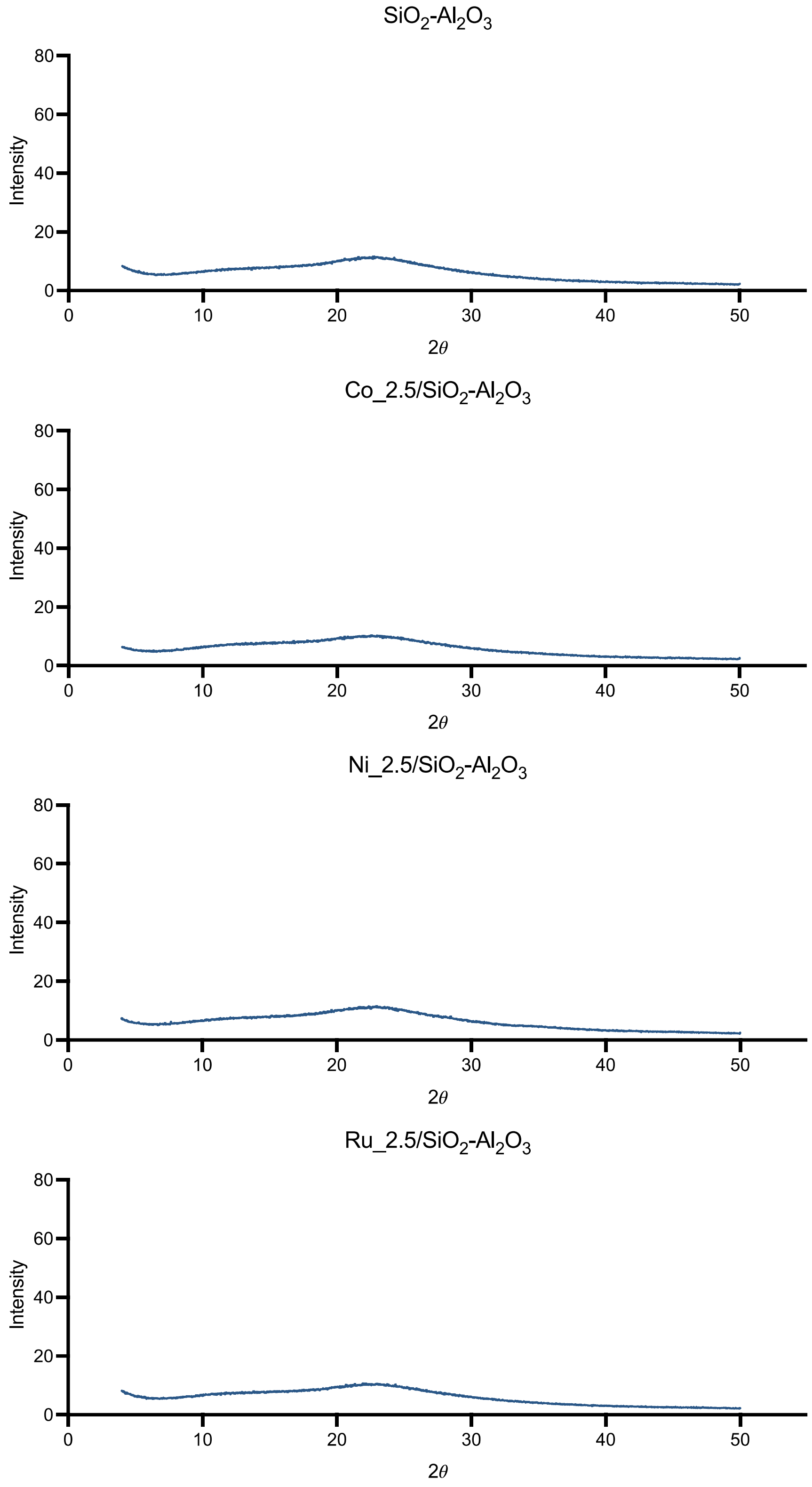


**Supplementary Figure 1 Powder X-ray of $SiO_2$-$Al_2O_3$-based catalysts.** Measurements of $SiO_2$-$Al_2O_3$, Co/$SiO_2$-$Al_2O_3$, Ni/$SiO_2$-$Al_2O_3$ and Ru/$SiO_2$-$Al_2O_3$ with $2\theta$ = 4-50 degree. Source data are provided as a Source Data file.

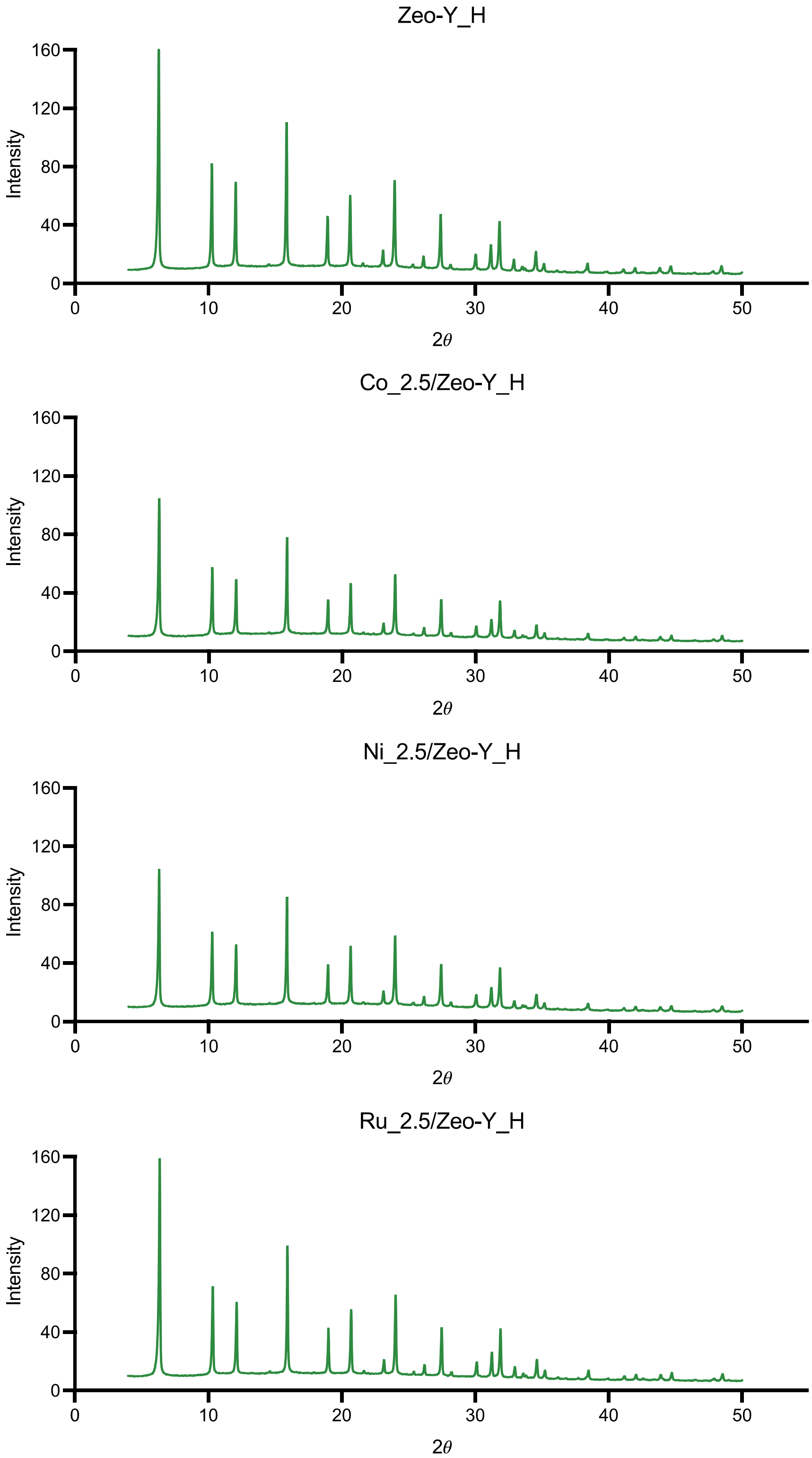


**Supplementary Figure 2 Powder X-ray of Zeo-Y_H-based catalysts.** Measurements of Zeo-Y_H, Co/Zeo-Y_H, Ni/Zeo-Y_H and Ru/Zeo-Y_H with 2$\theta$ = 4-50 degree. Source data are provided as a Source Data file.

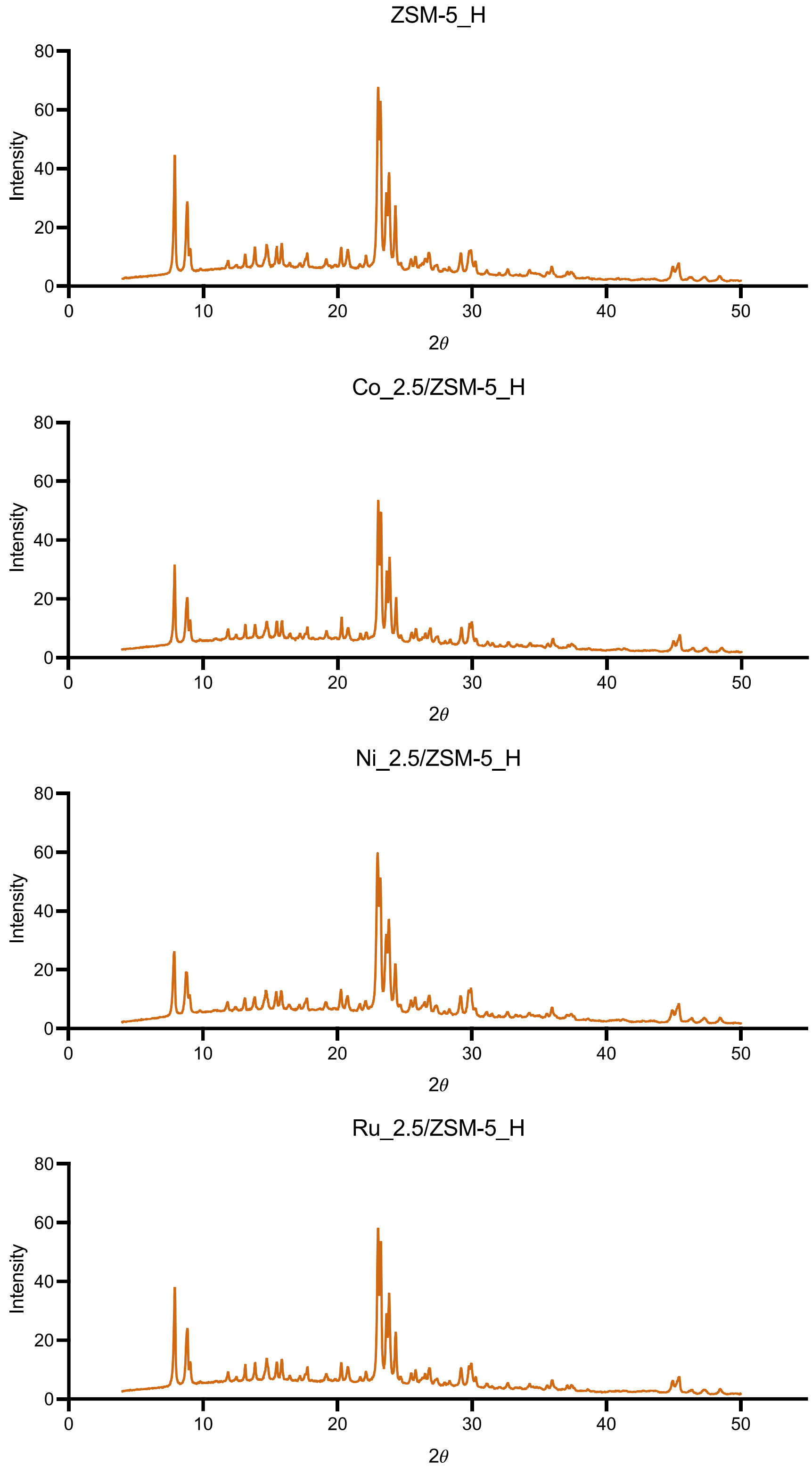


**Supplementary Figure 3 Powder X-ray of ZSM-5_H-based catalysts.** Measurements of ZSM-5_H, Co/ZSM-5_H, Ni/ZSM-5_H and Ru/ZSM-5_H with $2\theta$ = 4-50 degree. Source data are provided as a Source Data file.

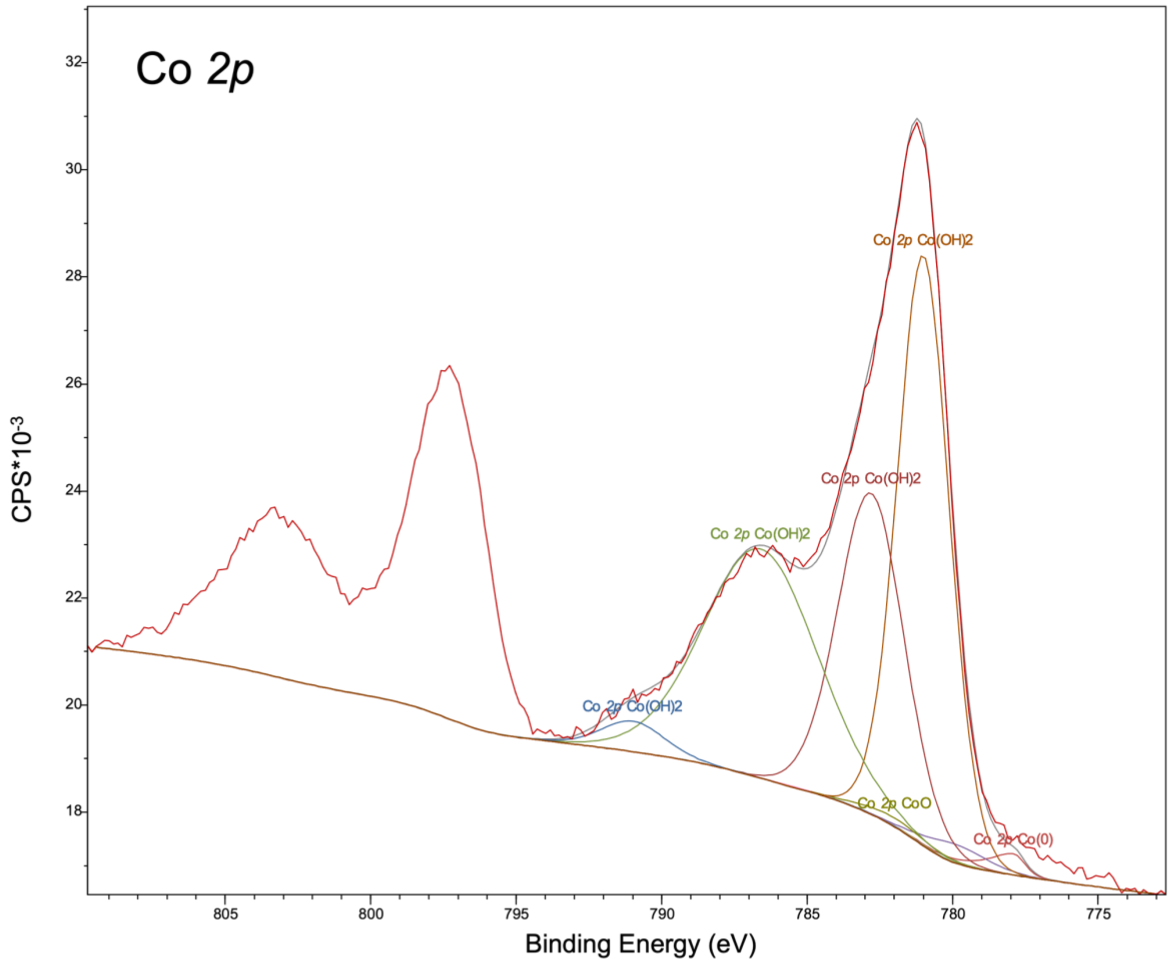


**Supplementary Figure 4 Curve fitted XPS analysis of Co *2p* region of Co/ZSM-5_H catalyst.** Fitting according to Mark Biesinger et al.[1] Source data are provided as a Source Data file.

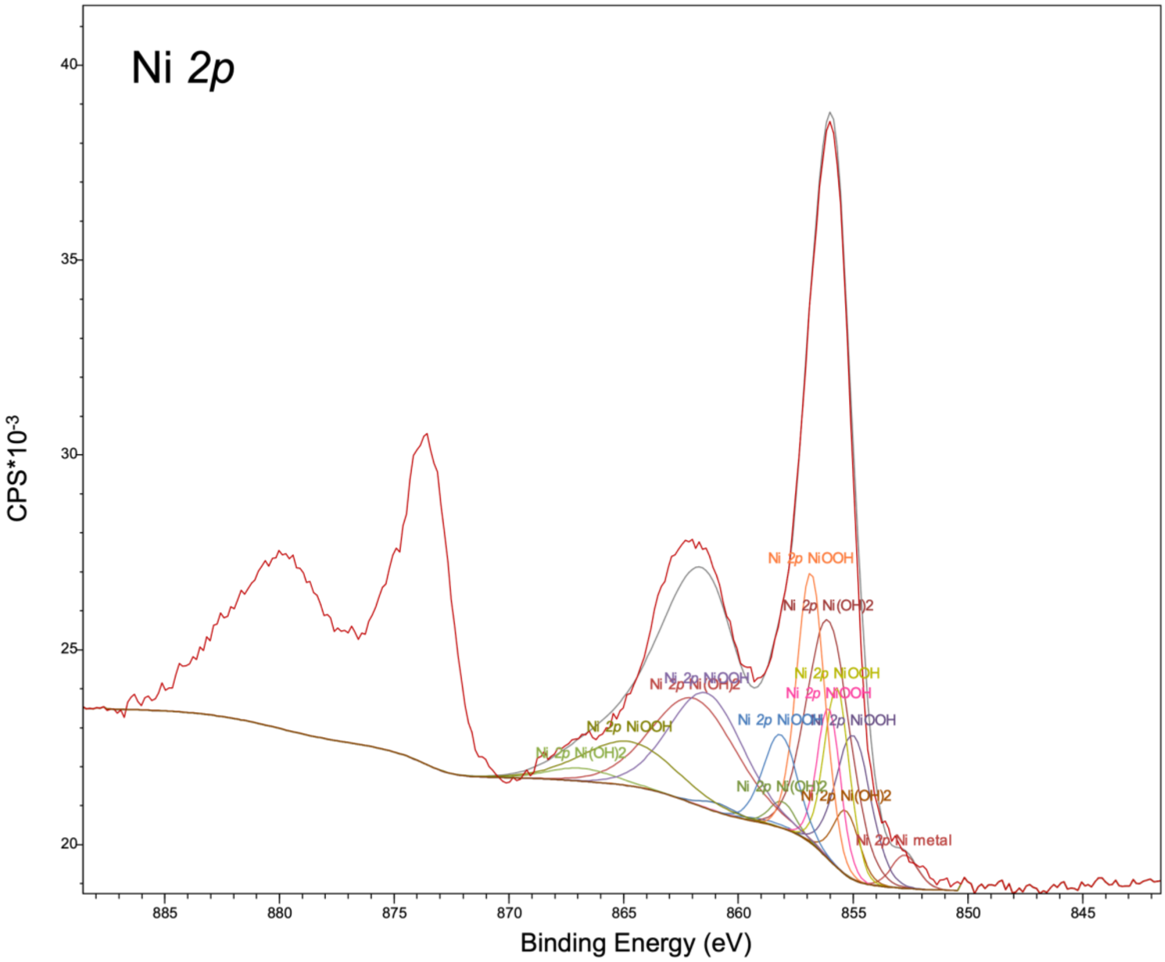


**Supplementary Figure 5 Curve fitted XPS analysis of Ni *2p* region of Ni/ZSM-5_H catalyst.** Fitting according to Mark Biesinger et al.[1] Source data are provided as a Source Data file.

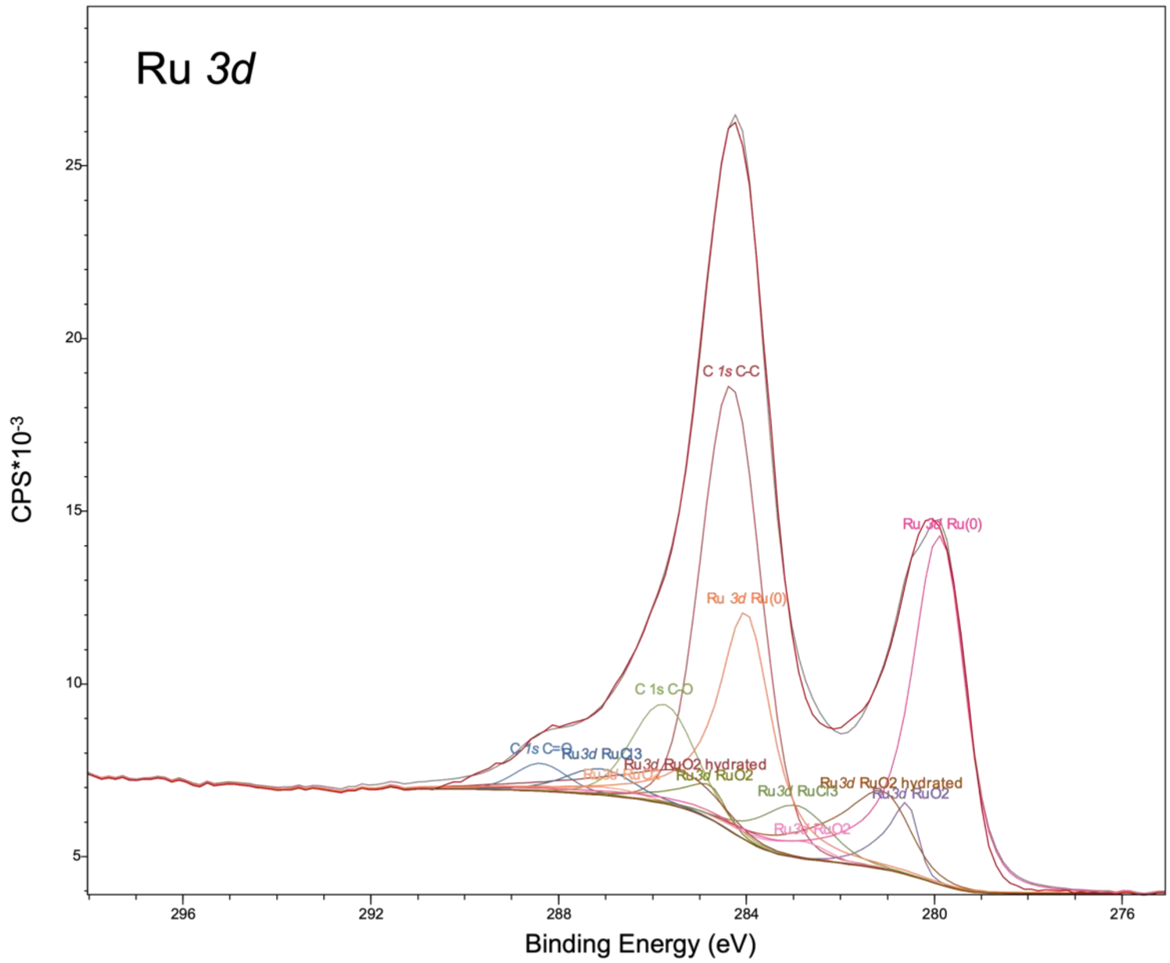


**Supplementary Figure 6 Curve fitted XPS analysis of Ru *3d* and C *1s* region of Ru/ZSM-5_H catalyst.** Fitting according to David J. Morgan.[2] Source data are provided as a Source Data file.

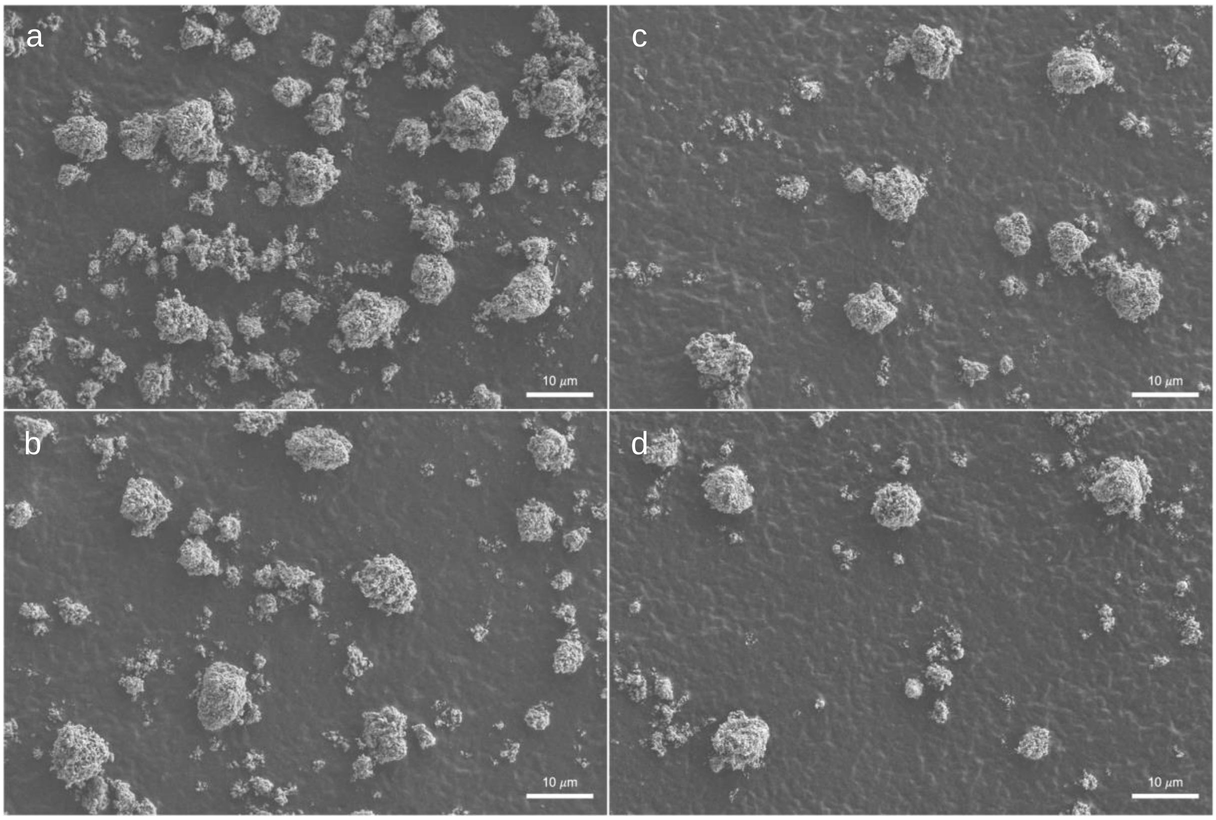


**Supplementary Figure 7 SEM images (scale bar = 10 μm) showing the particle distributions. a** ZSM-5_H (6.4-9.4 μm), **b** Co/ZSM-5_H (6.3-9.7 μm), **c** Ni/ZSM-5_H (6.3-8.6 μm) and **d** Ru/ZSM-5_H (6.0-10.4 μm).

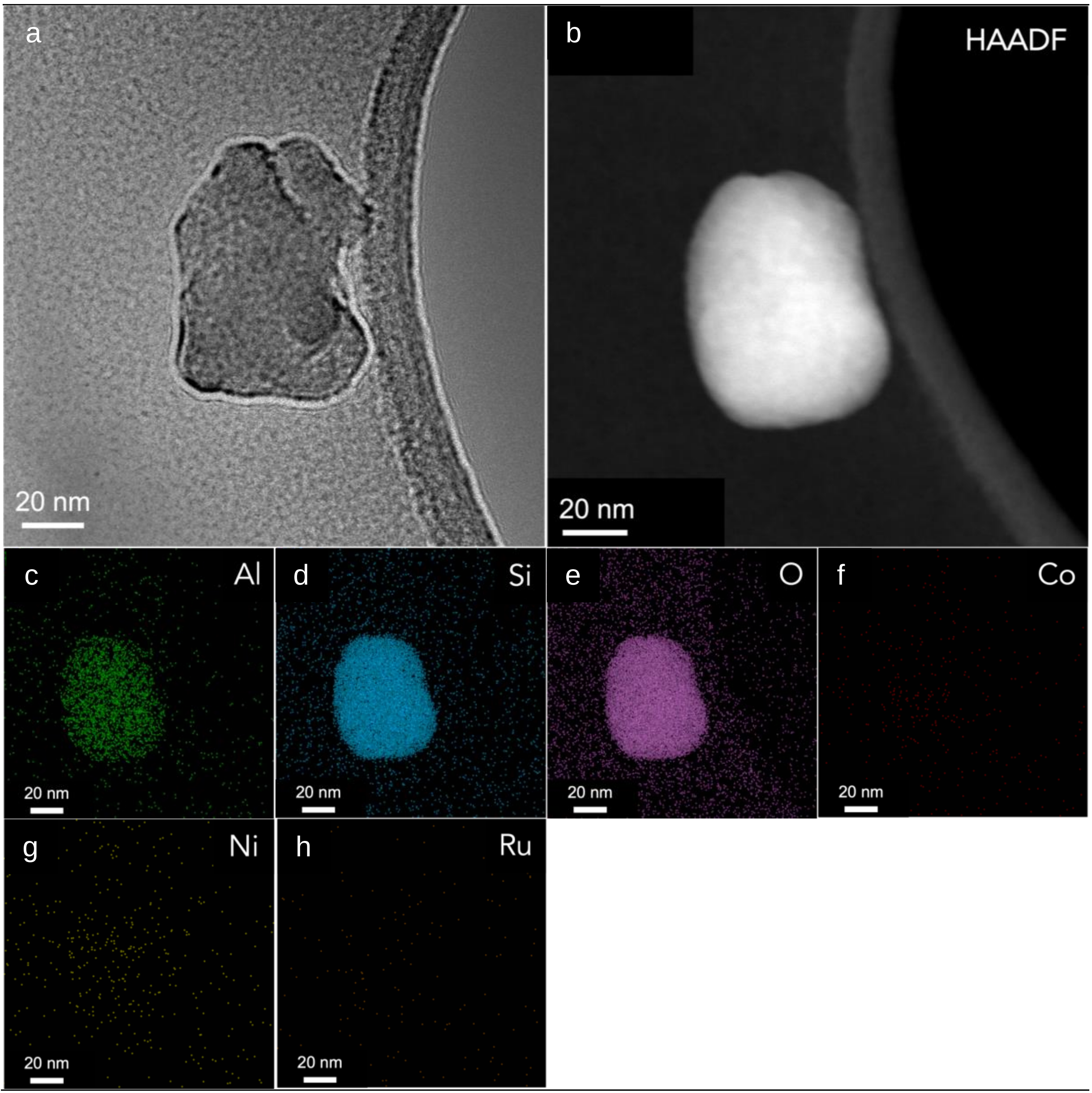


**Supplementary Figure 8 Electron microscopy images of ZSM-5_H.** TEM bright-field image (scale bar = 20 nm) of **a** ZSM-5_H. HAADF image (scale bar = 20 nm) of **b** ZSM-5_H. STEM-EDS elemental mapping of **c** Al, **d** Si, **e** O, **f** Co, **g** Ni and **h** Ru.

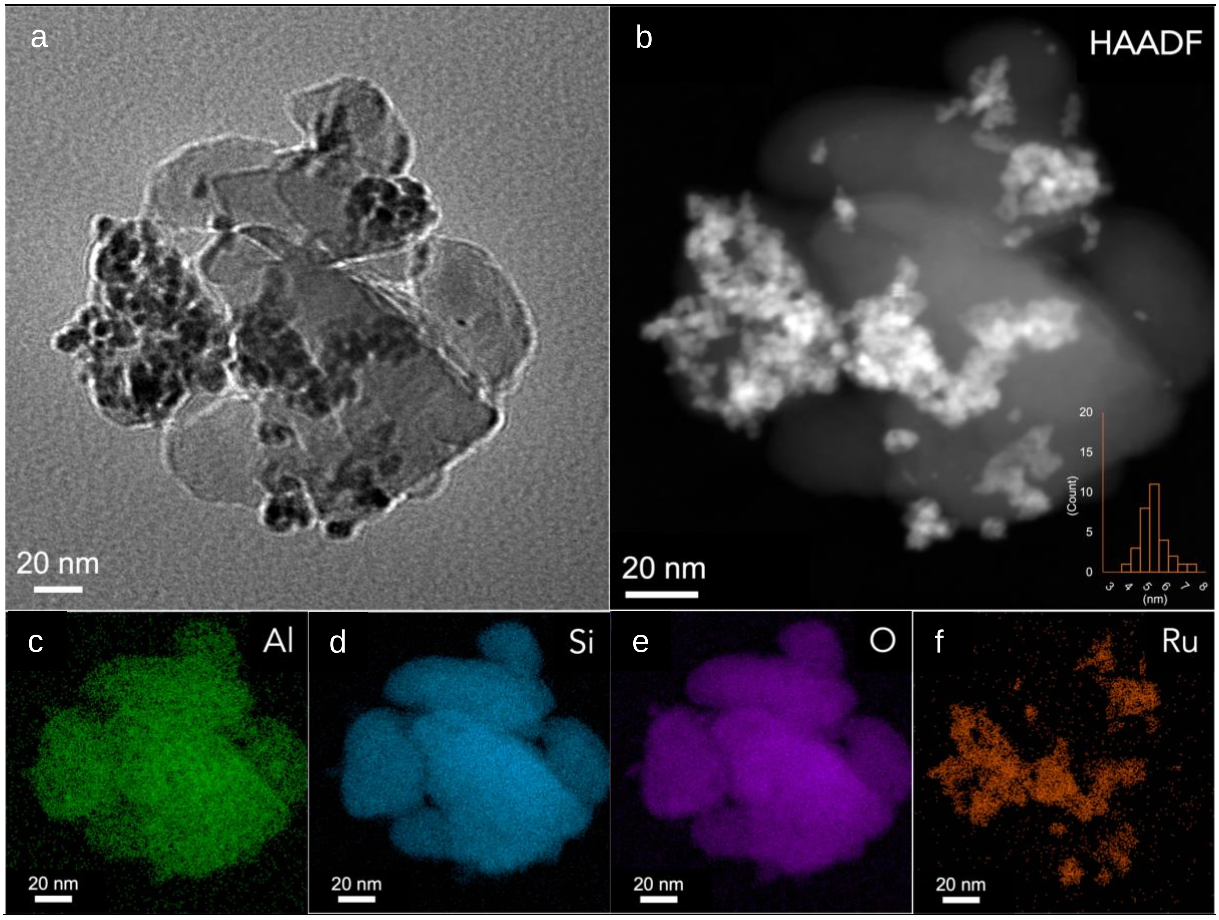


**Supplementary Figure 9 Electron microscopy images of Ru/ZSM-5_H.** TEM bright-field image (scale bar = 20 nm) of **a** Ru/ZSM-5_H. HAADF image (scale bar = 20 nm) of **b** Ru/ZSM-5_H with Ru NP distributions = 5.4±0.8 nm. STEM-EDS elemental mapping of **c** Al, **d** Si, **e** O and **f** Ru.

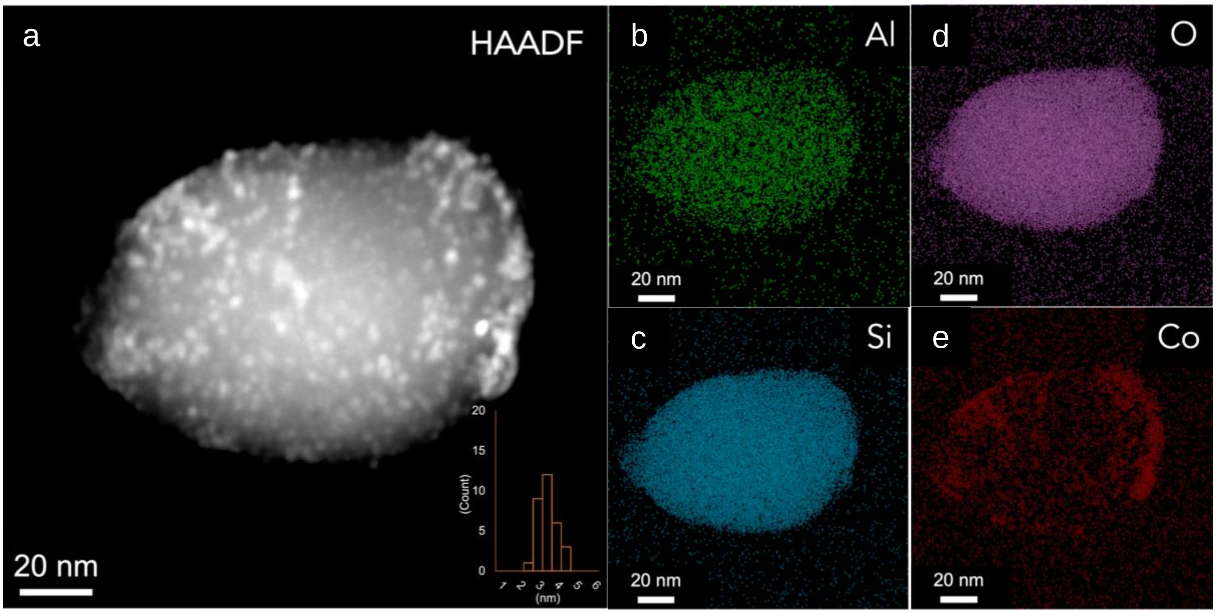


**Supplementary Figure 10 Electron microscopy images of Co/ZSM-5_H.** HAADF image (scale bar = 20 nm) of **a** Co/ZSM-5_H with Co NP distributions = 3.6±0.5 nm. STEM-EDS elemental mapping of **b** Al, **c** Si, **d** O and **e** Co.

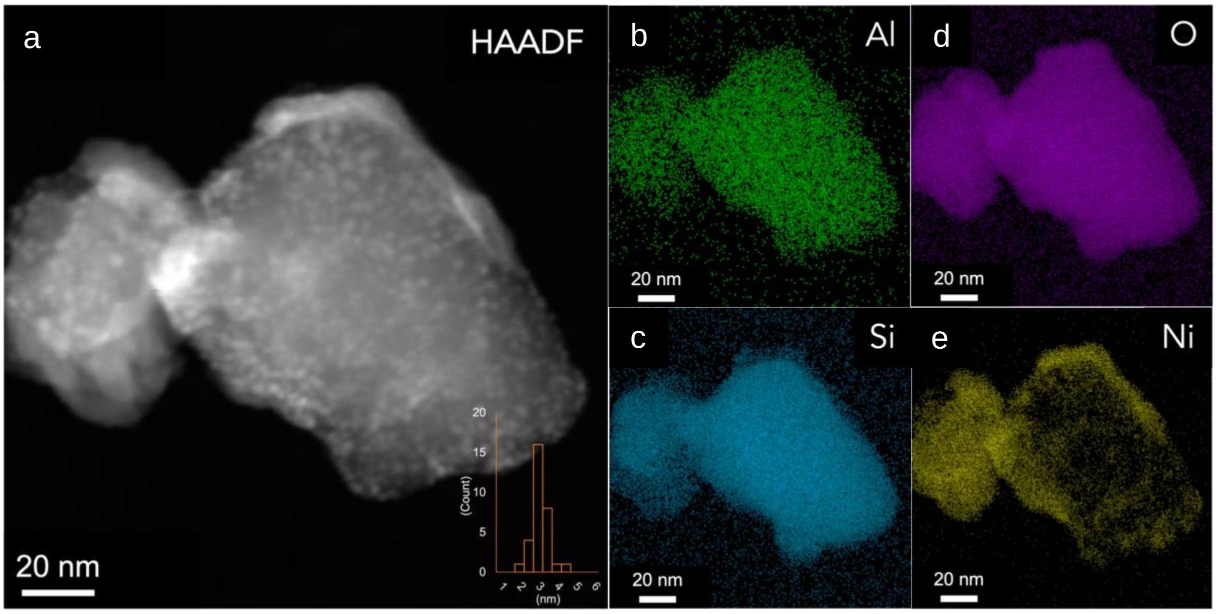


**Supplementary Figure 11 Electron microscopy images of Ni/ZSM-5_H.** HAADF image (scale bar = 20 nm) of **a** Ni/ZSM-5_H with Ni NP distributions = 3.1±0.4 nm. STEM-EDS elemental mapping of **b** Al, **c** Si, **d** O and **e** Ni.

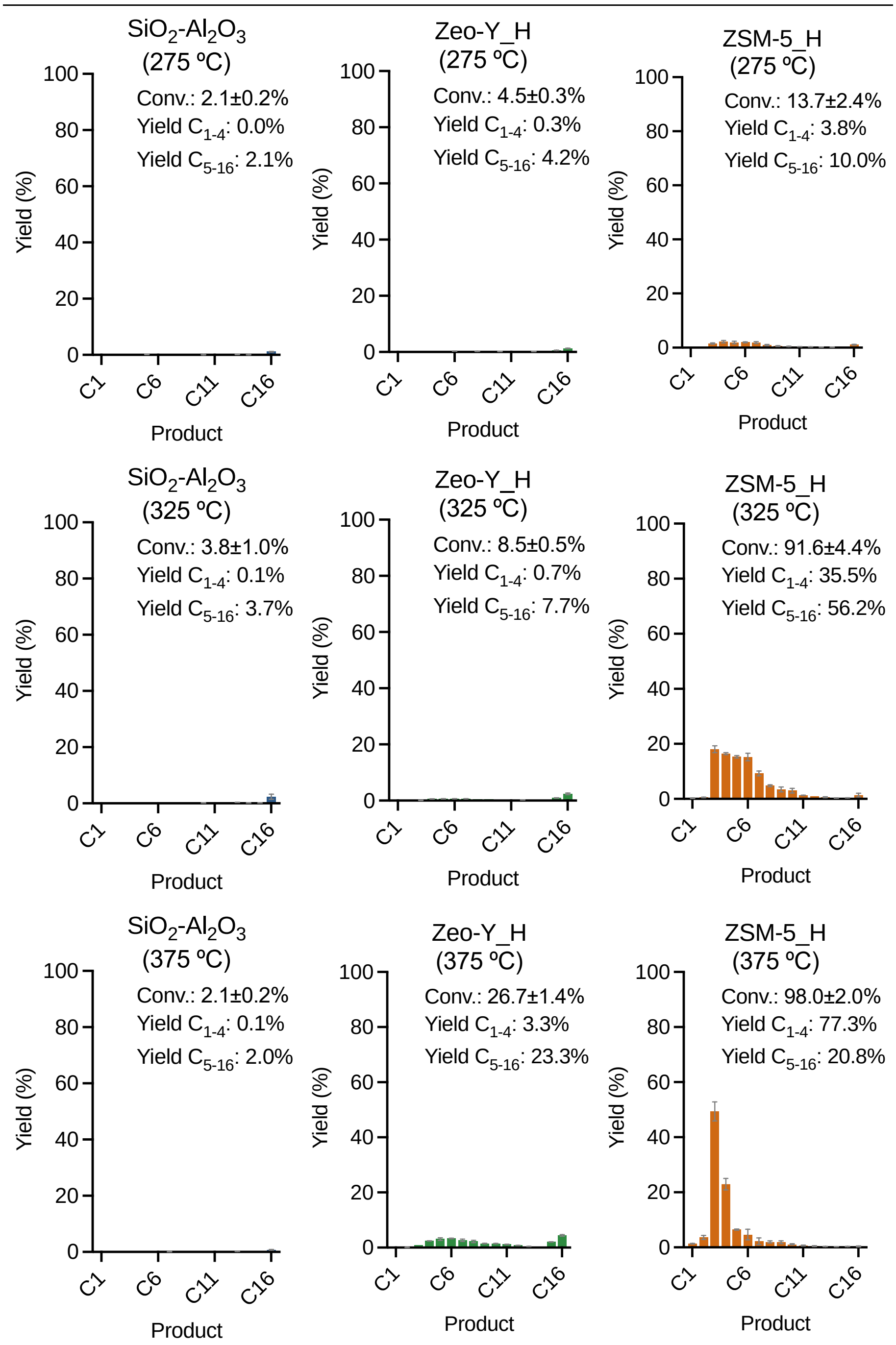


**Supplementary Figure 12 Product distributions after $nC_{16}$ (1.59 g) deconstructions.** In the presence of unmodified silica-alumina catalysts (0.1 g): $SiO_2$-$Al_2O_3$, Zeo-Y_H and ZSM-5_H, 45 bar $H_2$, 2 hrs. Note that $nC_{12}$ signal originated from the addition as an internal standard has been suppressed, and the yield of $C_{12}$ products was derived from the $nC_{16}$ substrate. Error bars = standard deviation. Source data are provided as a Source Data file.

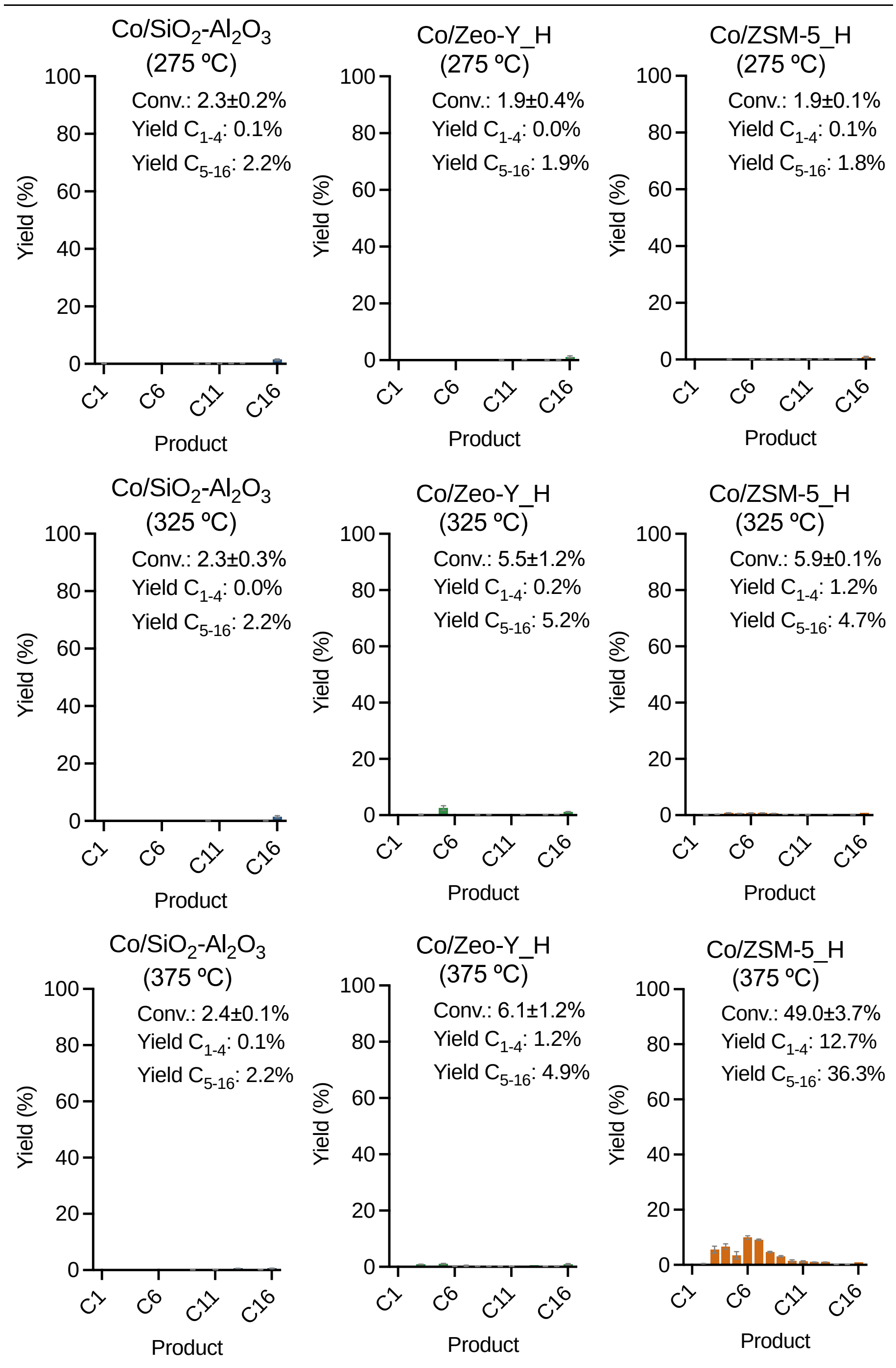


**Supplementary Figure 13 Product distributions after $nC_{16}$ (1.59 g) deconstructions.** In the presence of Co-modified catalysts (0.1 g, metal loading = 2.5 wt%): Co/$SiO_2$-$Al_2O_3$, Co/Zeo-Y_H and Co/ZSM-5_H, 45 bar $H_2$, 2 hrs. Note that $nC_{12}$ signal originated from the addition as an internal standard has been suppressed, and the yield of $C_{12}$ products was derived from the $nC_{16}$ substrate. Error bars = standard deviation. Source data are provided as a Source Data file.

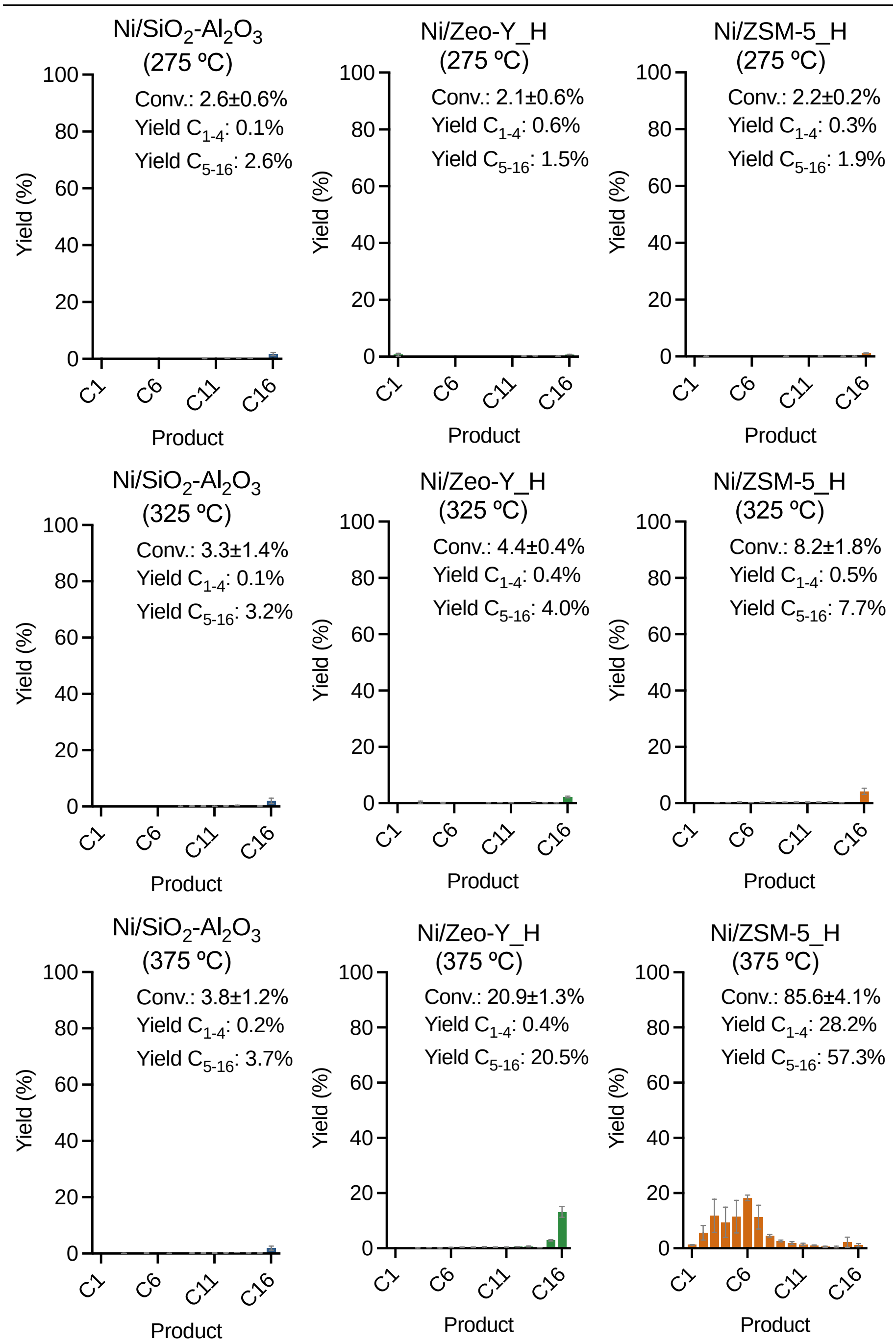


**Supplementary Figure 14 Product distributions after $nC_{16}$ (1.59 g) deconstructions.** In the presence of Ni-modified catalysts (0.1 g, metal loading = 2.5 wt%): Ni/$SiO_2$-$Al_2O_3$, Ni/Zeo-Y_H and Ni/ZSM-5_H, 45 bar $H_2$, 2 hrs. Note that $nC_{12}$ signal originated from the addition as an internal standard has been suppressed, and the yield of $C_{12}$ products was derived from the $nC_{16}$ substrate. Error bars = standard deviation. Source data are provided as a Source Data file.

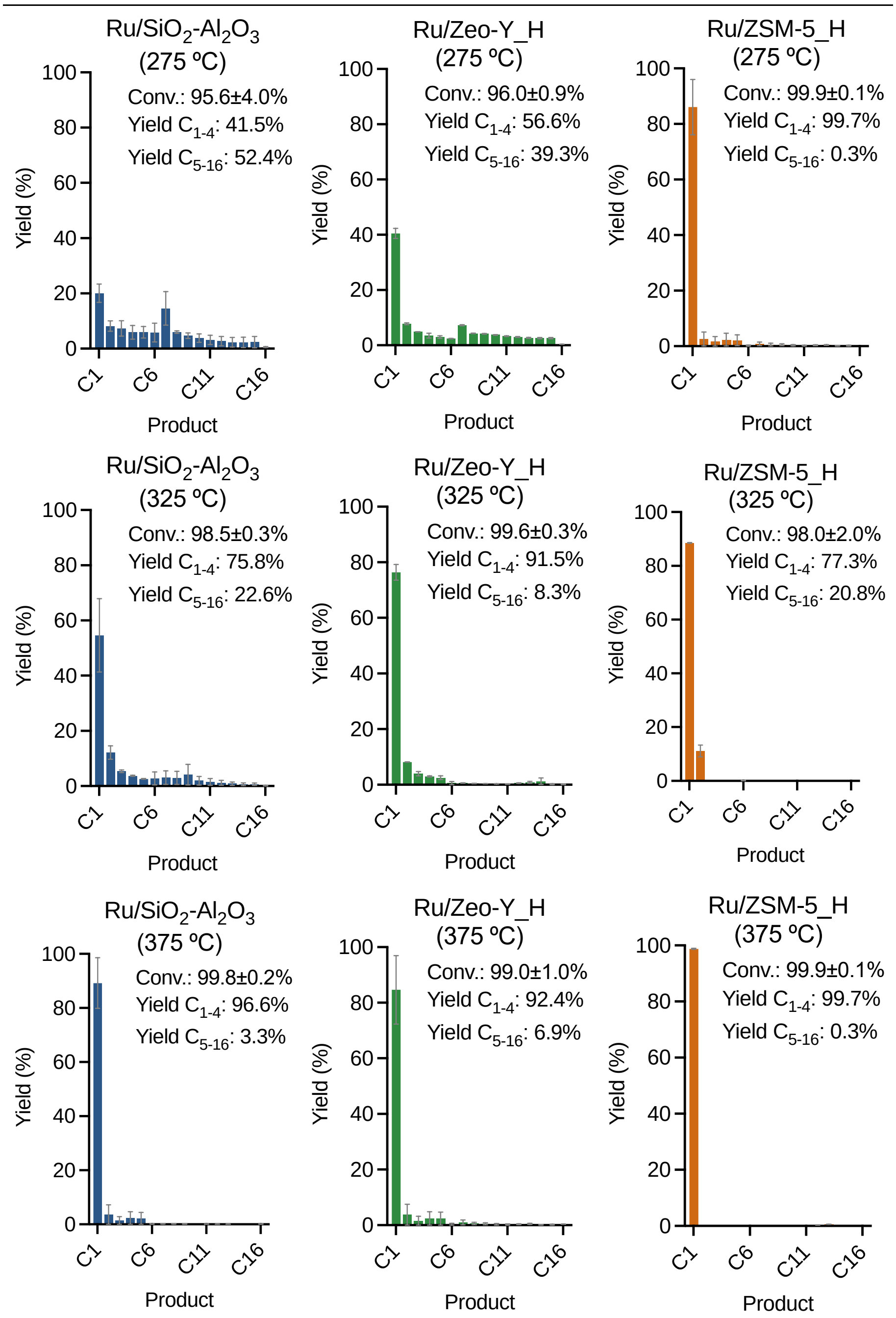


**Supplementary Figure 15 Product distributions after $nC_{16}$ (1.59 g) deconstructions.** In the presence of Ru-modified catalysts (0.1 g, metal loading = 2.5 wt%): Ru/$SiO_2$-$Al_2O_3$, Ru/Zeo-Y_H and Ru/ZSM-5_H, 45 bar $H_2$, 2 hrs. Note that $nC_{12}$ signal originated from the addition as an internal standard has been suppressed, and the yield of $C_{12}$ products was derived from the $nC_{16}$ substrate. Error bars = standard deviation. Source data are provided as a Source Data file.

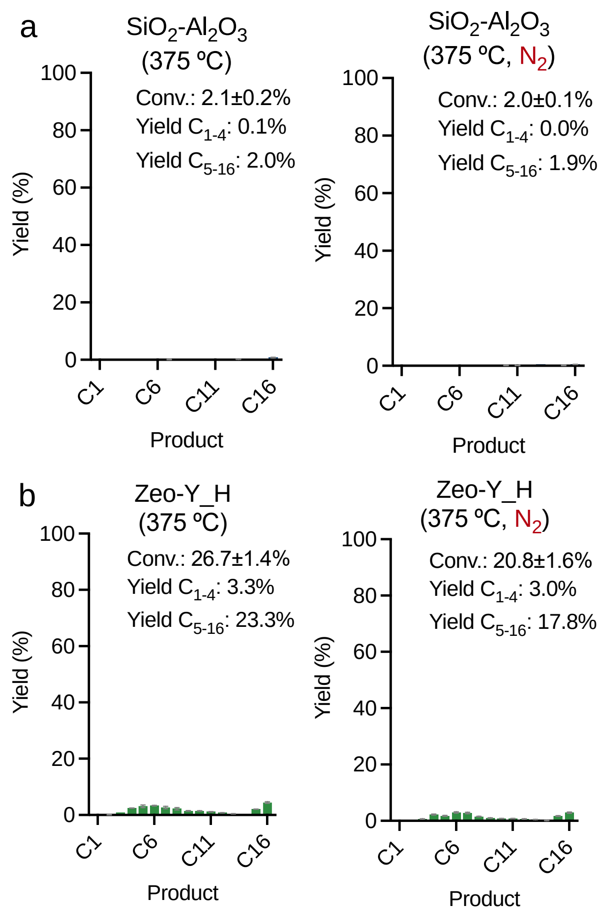


**Supplementary Figure 16 Product distributions after n$C_{16}$ (1.59 g) deconstructions.** In the presence of **a** $SiO_2$-$Al_2O_3$ (0.1 g) and **b** Zeo-Y_H (0.1 g) under 45 bar $H_2$ and $N_2$ at 375 ºC, 2 hrs. Note that n$C_{12}$ signal originated from the addition as an internal standard has been suppressed, and the yield of $C_{12}$ products was derived from the n$C_{16}$ substrate. Error bars = standard deviation. Source data are provided as a Source Data file.

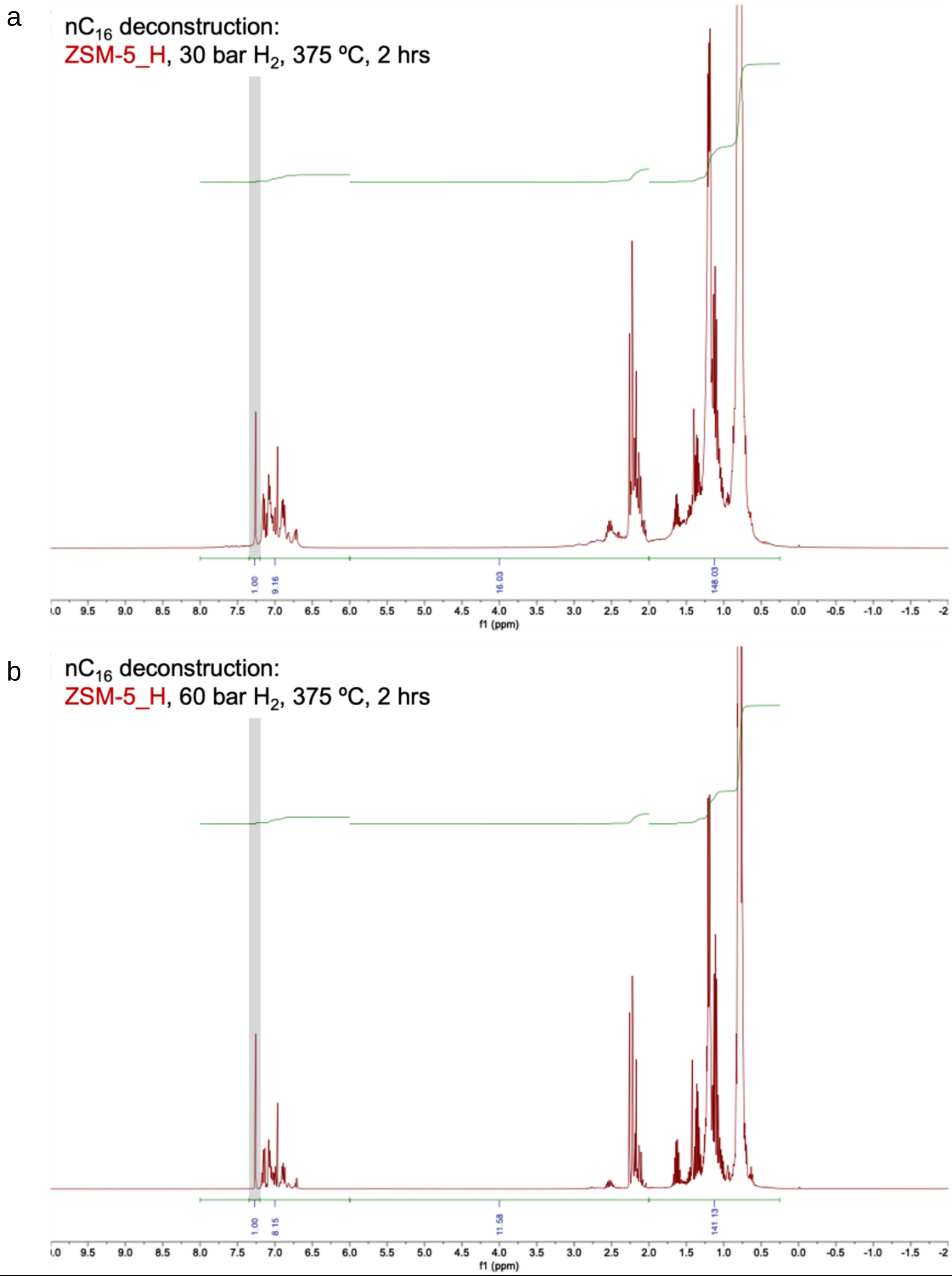


**Supplementary Figure 17 $^1$H NMR spectra of liquid products after $nC_{16}$ (1.59 g) deconstruction.** In the presence of ZSM-5_H (0.1 g) 375 ºC, 2 hrs under **a** 30 bar $H_2$, proton integration: 1.00, 9.16, 16.03, 148.03 = $CDCl_3$ (gray marked area, δ = 7.20-7.35), aromatic (δ = 6.0-8.0), unsaturated (δ = 2.0-6.0), saturated (δ = 0.25-2.0) and **b** 60 bar $H_2$, proton integration: 1.00, 8.15, 11.58, 141.13 = $CDCl_3$ (gray marked area, δ = 7.20-7.35), aromatic (δ = 6.0-8.0), unsaturated (δ = 2.0-6.0), saturated (δ = 0.25-2.0).

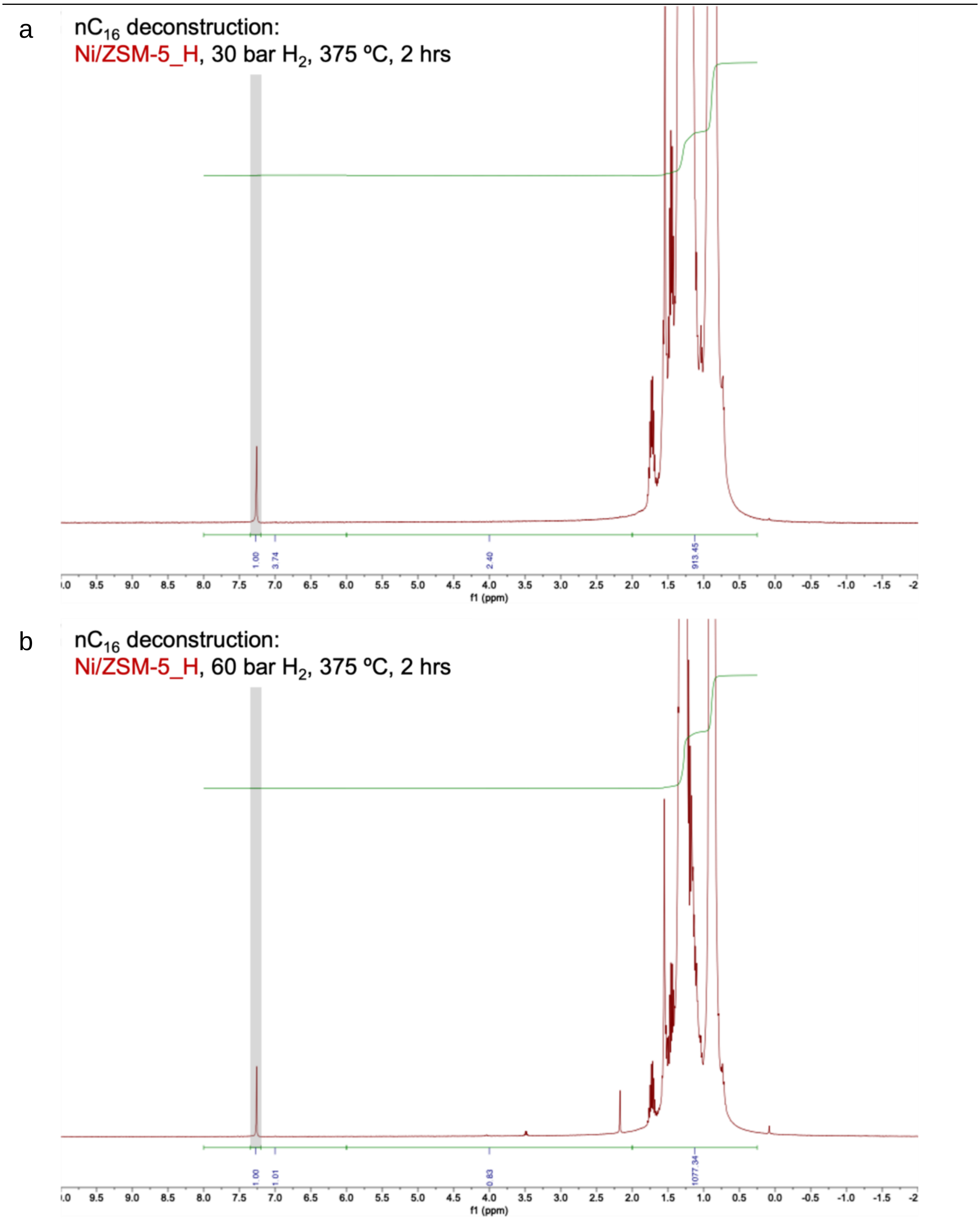


**Supplementary Figure 18 $^{1}H$ NMR spectra of liquid products after $nC_{16}$ (1.59 g) deconstruction.** In the presence of Ni/ZSM-5_H (0.1 g) 375 ºC, 2 hrs under **a** 30 bar $H_2$, proton integration: 1.00, 3.74, 2.40, 913.45 = $CDCl_3$ (gray marked area, δ = 7.20-7.35), aromatic (δ = 6.0-8.0), unsaturated (δ = 2.0-6.0), saturated (δ = 0.25-2.0) and **b** 60 bar $H_2$, proton integration: 1.00, 1.01, 0.83, 1077.34 = $CDCl_3$ (gray marked area, δ = 7.20-7.35), aromatic (δ = 6.0-8.0), unsaturated (δ = 2.0-6.0), saturated (δ = 0.25-2.0).

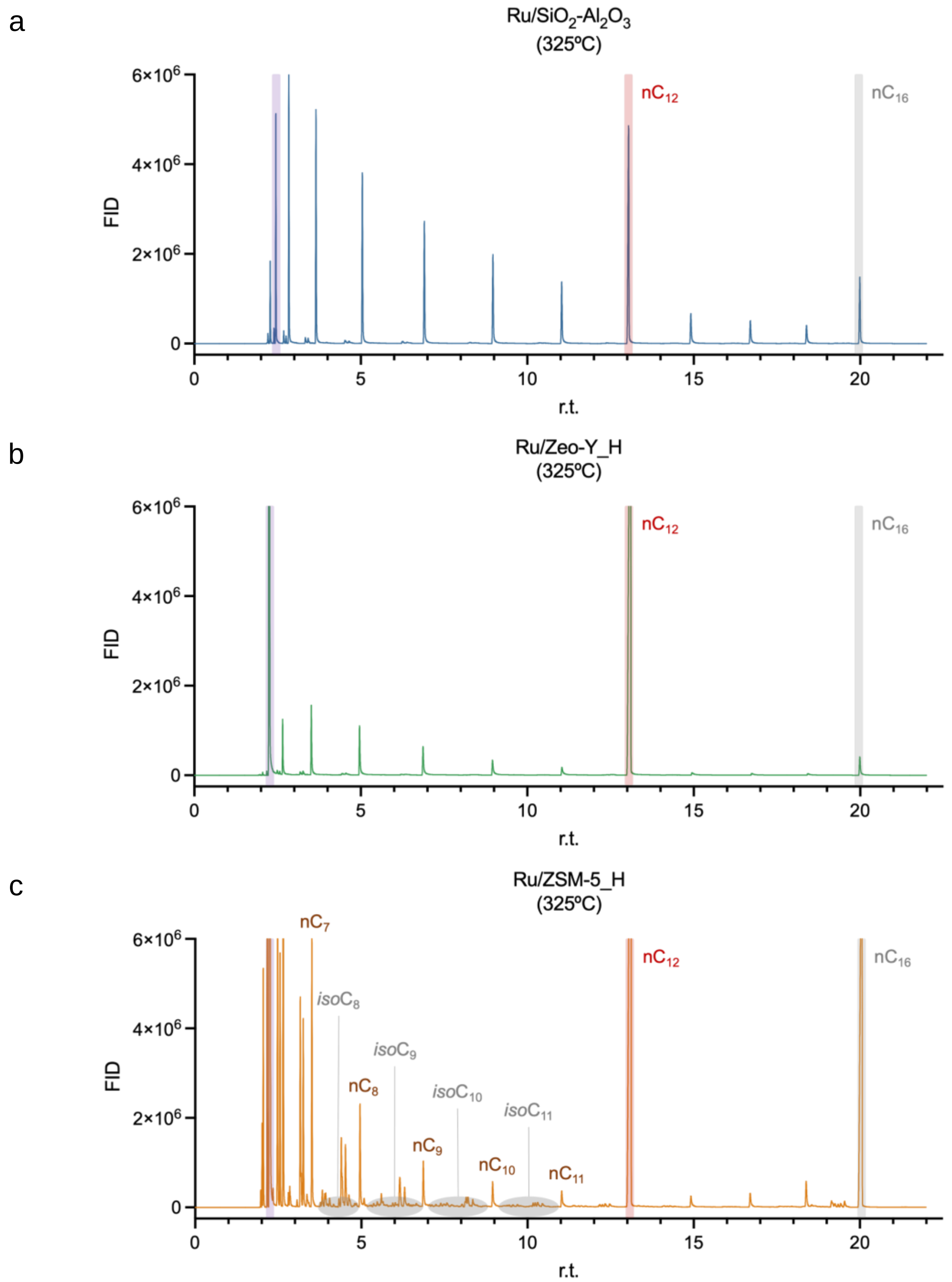


**Supplementary Figure 19 GC-FID traces of liquid products after the $nC_{16}$ (1.59 g) deconstruction.** In the presence of **a** Ru/$SiO_2$-$Al_2O_3$ (0.1 g, metal loading = 2.5 wt%), **b** Ru/Zeo-Y_H (0.1 g, metal loading = 2.5 wt%) and **c** Ru/ZSM-5_H (0.1 g, metal loading = 2.5 wt%) under 45 bar $H_2$ at 325 ºC, 2 hrs. Note that the peaks with retention time ~2.7 and ~14.1 min were diethyl ether (solvent for the GC sample) and $nC_{12}$ (internal standard), respectively.

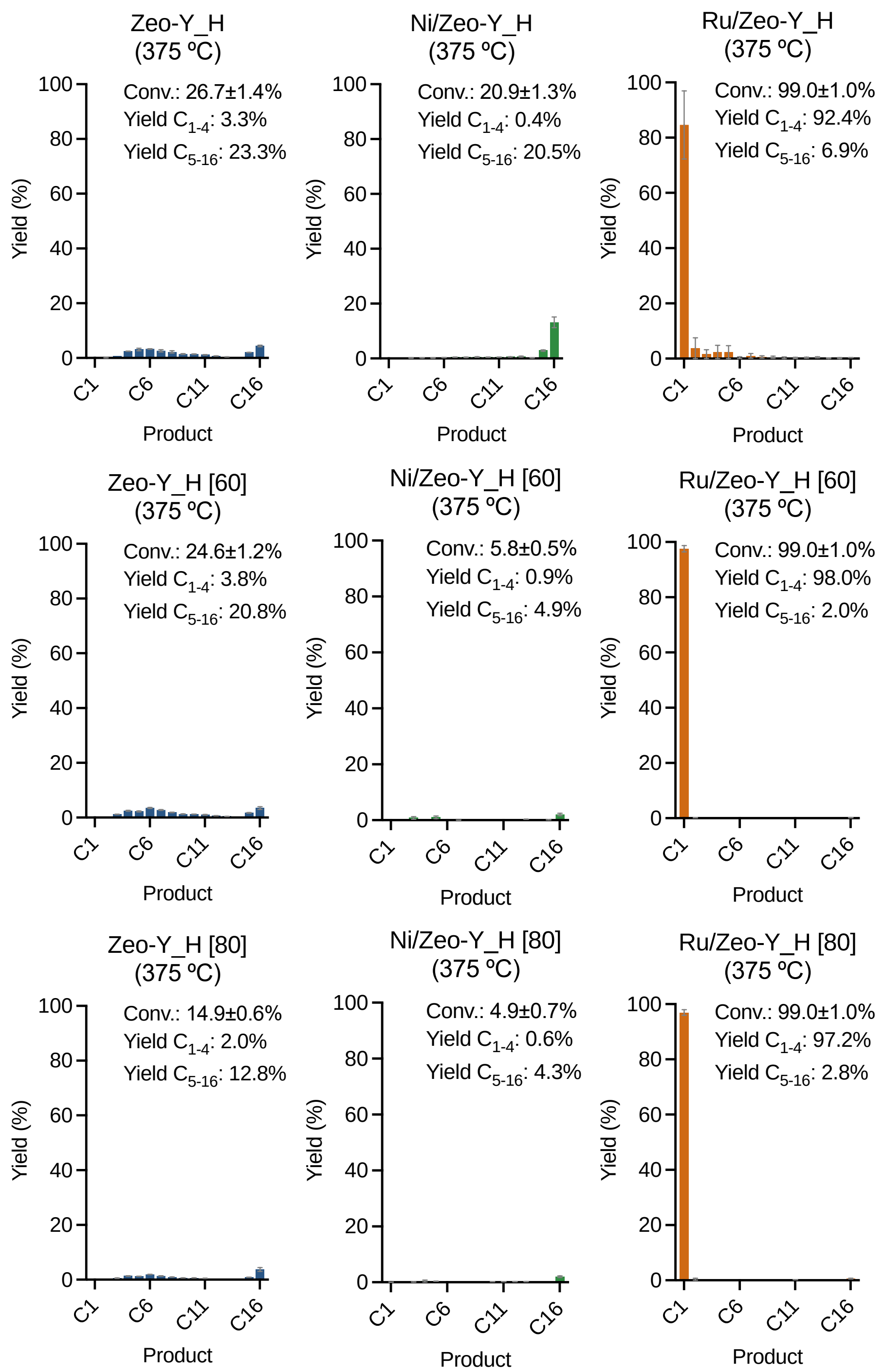


**Supplementary Figure 20 Product distributions after $nC_{16}$ (1.59 g) deconstructions.** In the presence of Zeo-Y_H-based catalysts with various Si/Al ratios (0.1 g, metal loading = 2.5 wt%): Zeo-Y_H, Zeo-Y_H [60], Zeo-Y_H [80], Ni/Zeo-Y_H, Ni/Zeo-Y_H [60], Ni/Zeo-Y_H [80], Ru/Zeo-Y_H, Ru/Zeo-Y_H [60], and Ru/Zeo-Y_H [80], 45 bar $H_2$, 2 hrs. Note that $nC_{12}$ signal originated from the addition as an internal standard has been suppressed, and the yield of $C_{12}$ products herein is derived from the $nC_{16}$ substrate. Error bars = standard deviation. Source data are provided as a Source Data file.

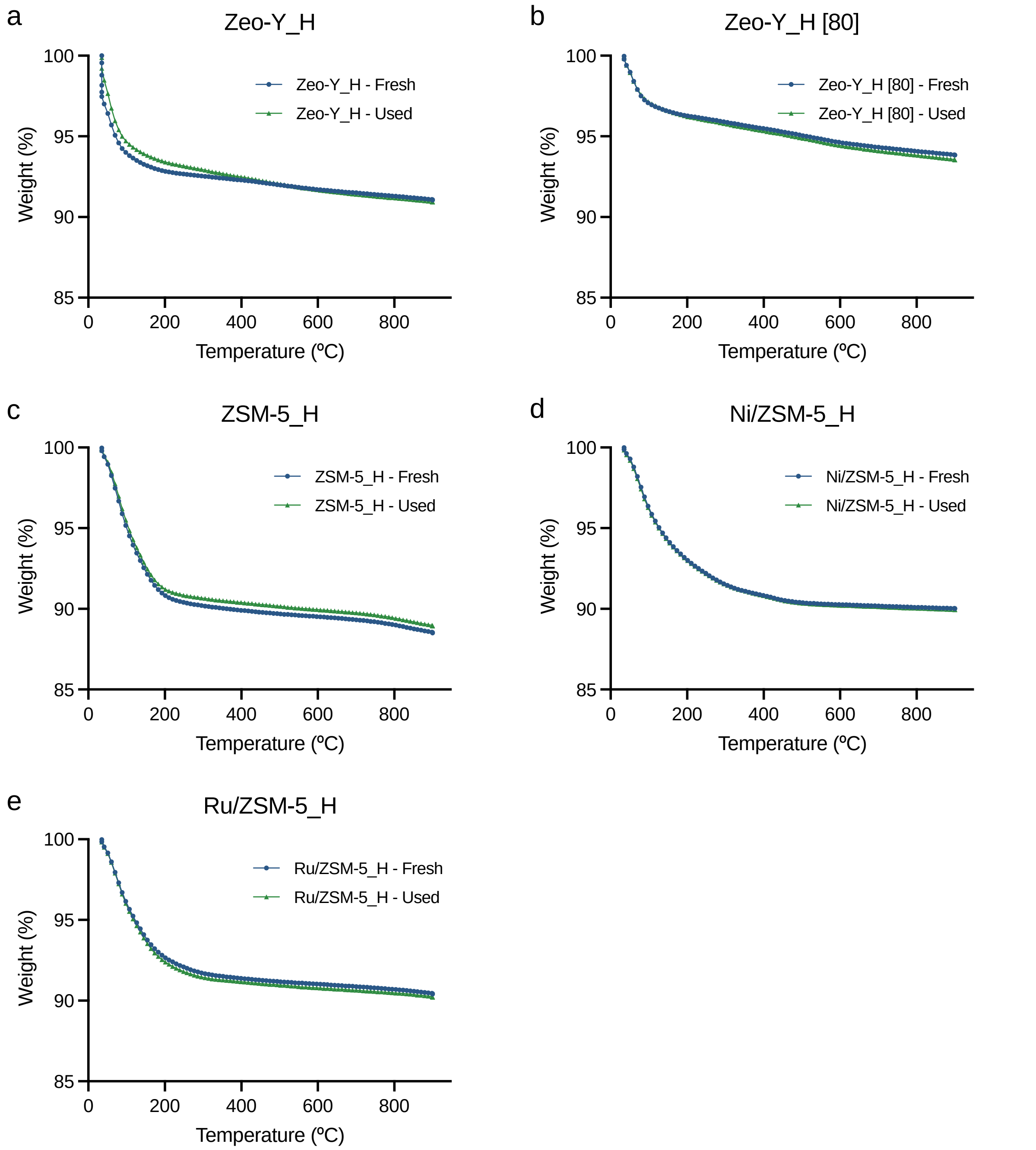


**Supplementary Figure 21 TGA analysis of fresh and used catalyst**. **a** Zeo-Y_H **b** Zeo-Y_H [80] **c** ZSM-5_H **d** Ni/ZSM-5_H **e** Ru/ZSM-5 _H with a ramping rate of 5 ºC/min from 35 to 900 ºC and a flow rate of 20 mL/min under air. Source data are provided as a Source Data file.

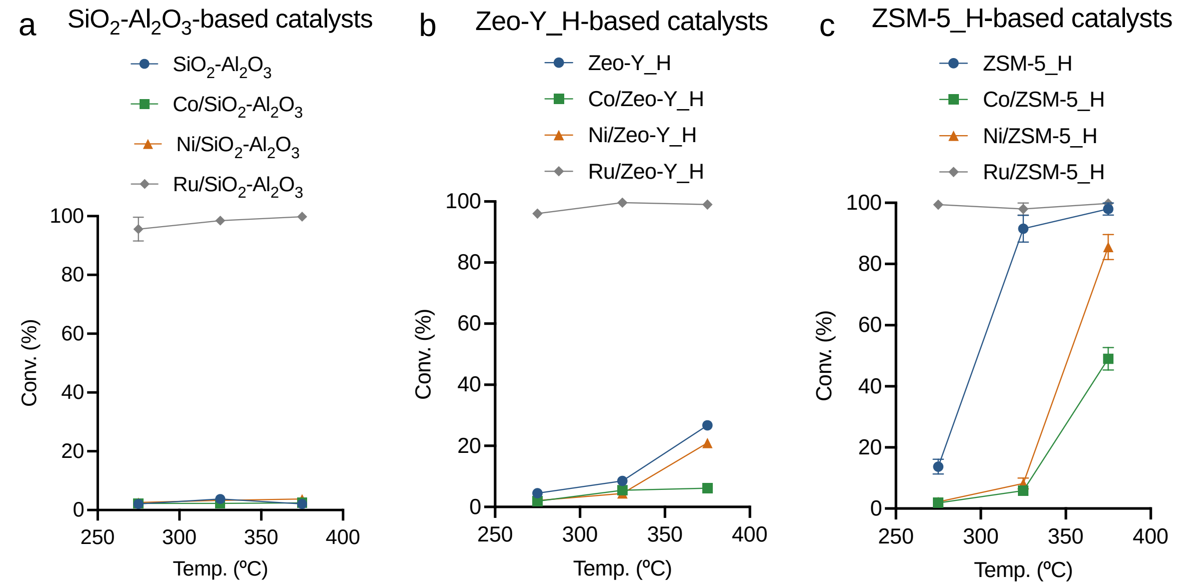


**Supplementary Figure 22 n$C_{16}$ (1.59 g) deconstructions with 45 bar $H_2$ at 275, 325 and 375 ºC, 2 hrs.** In the presence of **a** $SiO_2$-$Al_2O_3$-based catalysts (0.1 g, metal loading = 2.5 wt%): $SiO_2$-$Al_2O_3$, Co/$SiO_2$-$Al_2O_3$, Ni/$SiO_2$-$Al_2O_3$, Ru/$SiO_2$-$Al_2O_3$, **b** Zeo-Y_H-based catalysts (0.1 g, metal loading = 2.5 wt%): Zeo-Y_H, Co/Zeo-Y_H, Ni/Zeo-Y_H, Ru/Zeo-Y_H, **c** ZSM-5_H-based catalysts (0.1 g, metal loading = 2.5 wt%): ZSM-5_H, Co/ZSM-5_H, Ni/ZSM-5_H, Ru/ZSM-5_H. Error bars = standard deviation. Source data are provided as a Source Data file.

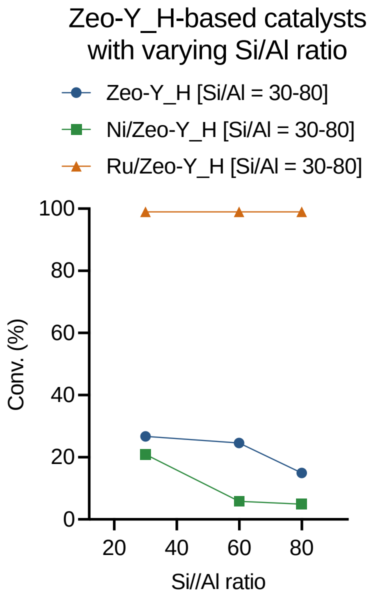


**Supplementary Figure 23 n$C_{16}$ (1.59 g) deconstructions with 45 bar $H_2$ at 375 ºC, 2 hrs.** In the presence of Zeo-Y_H-based catalysts with varying Si/Al ratios (0.1 g, metal loading = 2.5 wt%): Zeo-Y_H, Zeo-Y_H [60], Zeo-Y_H [80], Ni/Zeo-Y_H, Ni/Zeo-Y_H [60], Ni/Zeo-Y_H [80], Ru/Zeo-Y_H, Ru/Zeo-Y_H [60], and Ru/Zeo-Y_H [80]. Error bars = standard deviation. Source data are provided as a Source Data file.

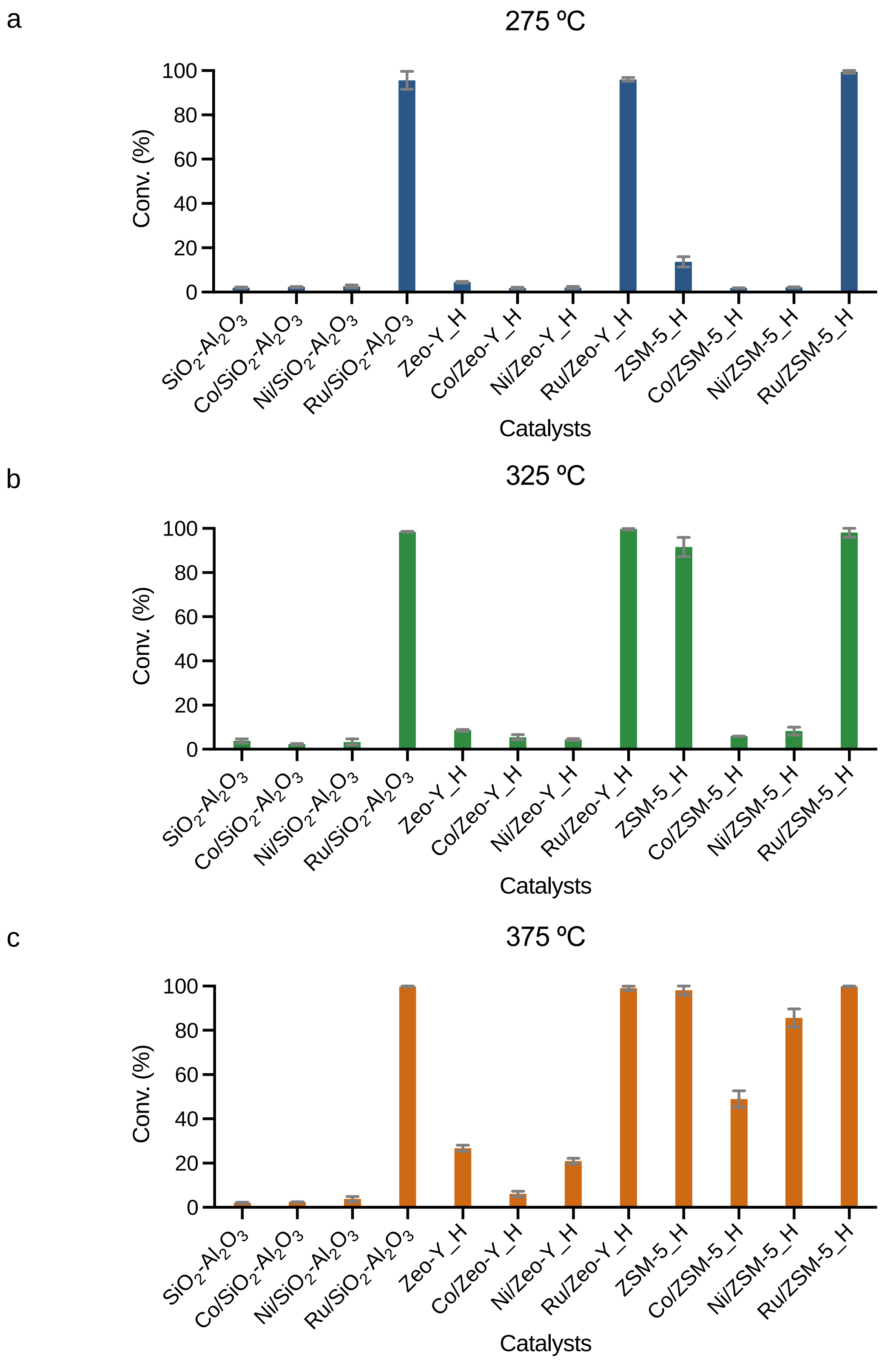


**Supplementary Figure 24 n$C_{16}$ (1.59 g) deconstruction with 45 bar $H_2$, 2 hrs.** In the presence of $SiO_2$-$Al_2O_3$, Co/$SiO_2$-$Al_2O_3$, Ni/$SiO_2$-$Al_2O_3$, Ru/$SiO_2$-$Al_2O_3$, Zeo-Y_H, Co/Zeo-Y_H, Ni/Zeo-Y_H, Ru/Zeo-Y_H, ZSM-5_H, Co/ZSM-5_H, Ni/ZSM-5_H and Ru/ZSM-5_H (cat. = 0.1 g, metal loading = 2.5 wt%) at **a** 275 ºC, **b** 325 ºC and **c** 375 ºC. Error bars = standard deviation. Source data are provided as a Source Data file.

**Supplementary Table 1** XPS surface relative atomic concentration of the ZSM-5_H-based catalysts.

| Catalyst | Si% (*2p*) | Al% (*2p*) | O% (*1s*) | Co% (*2p*) | Ni% (*2p*) | Ru% (*3d*) |
|---|---|---|---|---|---|---|
| ZSM-5_H | 28.6 | 2.8 | 68.7 | - | - | - |
| Co/ZSM-5_H | 22.4 | 0.8 | 67.0 | 9.8 | - | - |
| Ni/ZSM-5_H | 22.3 | 4.8 | 64.6 | - | 8.3 | - |
| Ru/ZSM-5_H | 26.6 | 3.2 | 67.6 | - | - | 2.6 |

**Supplementary Table 2** XPS surface species and their relative concentrations of the ZSM-5_H-based catalysts.

| Catalyst | Specie % | | | |
|---|---|---|---|---|
| Co/ZSM-5_H | Co(0)% (*2p*) | CoO% (*2p*) | $Co(OH)_2$% (*2p*) | |
| | 1.4 | 2.2 | 96.4 | |
| Ni/ZSM-5_H | Ni(0)% (*2p*) | NiO% (*2p*) | Ni(O)OH% (*2p*) | $Ni(OH)_2$% (*2p*) |
| | 1.8 | 0.3 | 60.4 | 37.5 |
| Ru/ZSM-5_H | Ru(0)% (*3d*) | $RuO_2$% (*3d*) | $RuO_2 \cdot H_2O$% (*3d*) | $RuCl_3$% (*3d*) |
| | 86.0 | 3.9 | 6.7 | 3.4 |

**Supplementary Table 3** *n*-Hexadecane deconstructions with the 12 catalysts from the main library at 275, 325, and 375 ºC including the carbon balance and hydrogen consumption.

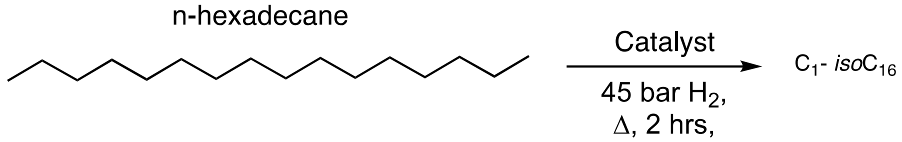


| Entry | Catalyst | Temp. (ºC) | Conv. (%) [g] | $C_{1-4}$ Yield (%) [g] | $C_{5-16}$ Yield (%) [g] | $H_2$ Cons. (%) [g] |
|---|---|---|---|---|---|---|
| 1 | $SiO_2$-$Al_2O_3$ | 275 ºC | 2.1±0.2 [0.03±0.00] | 0.0 [0.00] | 2.1 [0.03] | 1 [0.00] |
| 2 | $SiO_2$-$Al_2O_3$ | 325 ºC | 3.8±1.0 [0.06±0.02] | 0.1 [0.00] | 3.7 [0.06] | 6 [0.01] |
| 3 | $SiO_2$-$Al_2O_3$ | 375 ºC | 2.1±0.2 [0.03±0.00] | 0.1 [0.00] | 2.0 [0.03] | 5 [0.01] |
| 4 | Zeo-Y_H | 275 ºC | 4.5±0.3 [0.07±0.00] | 0.3 [0.01] | 4.2 [0.07] | 2 [0.00] |
| 5 | Zeo-Y_H | 325 ºC | 8.5±0.5 [0.14±0.01] | 0.7 [0.01] | 7.7 [0.12] | 10 [0.02] |
| 6 | Zeo-Y_H | 375 ºC | 26.7±1.4 [0.42±0.02] | 3.3 [0.05] | 23.3 [0.37] | 11 [0.03] |
| 7 | ZSM-5_H | 275 ºC | 13.7±2.4 [0.22±0.04] | 3.8 [0.06] | 10.0 [0.16] | 5 [0.01] |
| 8 | ZSM-5_H | 325 ºC | 91.6±4.4 [1.46±0.07] | 35.5 [0.58] | 56.2 [0.90] | 17 [0.04] |
| 9 | ZSM-5_H | 375 ºC | 98.0±2.0 [1.56±0.03] | 77.3 [1.27] | 20.8 [0.33] | 23 [0.06] |
| 10 | Co/$SiO_2$-$Al_2O_3$ | 275 ºC | 2.3±0.2 [0.04±0.00] | 0.1 [0.00] | 2.2 [0.03] | 4 [0.01] |
| 11 | Co/$SiO_2$-$Al_2O_3$ | 325 ºC | 2.3±0.3 [0.04±0.00] | 0.0 [0.00] | 2.2 [0.03] | 2 [0.00] |
| 12 | Co/$SiO_2$-$Al_2O_3$ | 375 ºC | 2.4±0.1 [0.04±0.00] | 0.1 [0.00] | 2.2 [0.03] | 7 [0.02] |
| 13 | Co/Zeo-Y_H | 275 ºC | 1.9±0.4 [0.03±0.01] | 0.0 [0.00] | 1.9 [0.03] | 4 [0.01] |
| 14 | Co/Zeo-Y_H | 325 ºC | 5.5±1.2 [0.09±0.02] | 0.2 [0.00] | 5.2 [0.08] | 6 [0.01] |
| 15 | Co/Zeo-Y_H | 375 ºC | 6.1±1.2 [0.10±0.02] | 1.2 [0.02] | 4.9 [0.08] | 8 [0.02] |
| 16 | Co/ZSM-5_H | 275 ºC | 1.9±0.1 [0.03±0.00] | 0.1 [0.00] | 1.8 [0.03] | 6 [0.01] |
| 17 | Co/ZSM-5_H | 325 ºC | 5.9±0.1 [0.09±0.00] | 1.2 [0.02] | 4.7 [0.07] | 6 [0.01] |
| 18 | Co/ZSM-5_H | 375 ºC | 49.0±3.7 [0.78±0.06] | 12.7 [0.21] | 36.3 [0.58] | 13 [0.03] |
| 19 | Ni/$SiO_2$-$Al_2O_3$ | 275 ºC | 2.6±0.6 [0.04±0.01] | 0.1 [0.00] | 2.6 [0.04] | 3 [0.01] |
| 20 | Ni/$SiO_2$-$Al_2O_3$ | 325 ºC | 3.3±1.4 [0.05±0.02] | 0.1 [0.00] | 3.2 [0.05] | 4 [0.01] |
| 21 | Ni/$SiO_2$-$Al_2O_3$ | 375 ºC | 3.8±1.2 [0.06±0.02] | 0.2 [0.00] | 3.7 [0.06] | 7 [0.02] |
| 22 | Ni/Zeo-Y_H | 275 ºC | 2.1±0.6 [0.03±0.01] | 0.6 [0.01] | 1.5 [0.02] | 4 [0.01] |
| 23 | Ni/Zeo-Y_H | 325 ºC | 4.4±0.4 [0.07±0.01] | 0.4 [0.01] | 4.0 [0.06] | 5 [0.01] |
| 24 | Ni/Zeo-Y_H | 375 ºC | 20.9±1.3 [0.33±0.02] | 0.4 [0.01] | 20.5 [0.31] | 8 [0.02] |
| 25 | Ni/ZSM-5_H | 275 ºC | 2.2±0.2 [0.03±0.00] | 0.3 [0.00] | 1.9 [0.03] | 4 [0.01] |
| 26 | Ni/ZSM-5_H | 325 ºC | 8.2±1.8 [0.13±0.03] | 0.5 [0.01] | 7.7 [0.12] | 7 [0.02] |
| 27 | Ni/ZSM-5_H | 375 ºC | 85.6±4.1 [1.36±0.07] | 28.2 [0.46] | 57.3 [0.92] | 13 [0.03] |
| 28 | Ru/$SiO_2$-$Al_2O_3$ | 275 ºC | 95.6±4.0 [1.52±0.06] | 41.5 [0.71] | 54.2 [0.86] | 27 [0.07] |
| 29 | Ru/$SiO_2$-$Al_2O_3$ | 325 ºC | 98.5±0.3 [1.57±0.00] | 75.8 [1.33] | 22.6 [0.36] | 60 [0.14] |
| 30 | Ru/$SiO_2$-$Al_2O_3$ | 375 ºC | 99.8±0.2 [1.59±0.00] | 96.6 [1.72] | 3.3 [0.05] | 83 [0.20] |
| 31 | Ru/Zeo-Y_H | 275 ºC | 96.0±0.9 [1.53±0.01] | 56.6 [0.99] | 39.3 [0.63] | 44 [0.11] |
| 32 | Ru/Zeo-Y_H | 325 ºC | 99.6±0.3 [1.58±0.00] | 91.5 [1.62] | 8.3 [0.13] | 73 [0.18] |
| 33 | Ru/Zeo-Y_H | 375 ºC | 99.0±1.0 [1.57±0.02] | 92.4 [1.65] | 6.9 [0.11] | 85 [0.21] |
| 34 | Ru/ZSM-5_H | 275 ºC | 99.4±0.6 [1.58±0.01] | 92.8 [1.65] | 6.6 [0.10] | 54 [0.13] |
| 35 | Ru/ZSM-5_H | 325 ºC | 98.0±2.0 [1.56±0.03] | 99.7 [1.78] | 0.3 [0.01] | 88 [0.21] |
| 36 | Ru/ZSM-5_H | 375 ºC | 99.8±0.2 [1.59±0.00] | 98.8 [1.77] | 1.1 [0.02] | 88 [0.21] |

Reaction conditions: *n*-hexadecane (1.59 g, 7.0 mmol), catalyst (0.1 g, metal loading = 2.5 wt%), S/C ratio (substrate/catalyst weight ratio) ~16, 45 bar $H_2$, 2 hrs. * All yields were calculated as the carbon yield and isomerized $C_{16}$ (*iso*$C_{16}$) are considered as products. Note that ~87% $H_2$ consumption (~105.0 mmol) is able to produce methane quantitatively due to the ~1.15 eq. $H_2$ stichometry.

**Supplementary Table 4** *n*-Hexadecane deconstruction using the Zeo-Y_H-based catalysts with varying SARs including the carbon balance and hydrogen consumption.

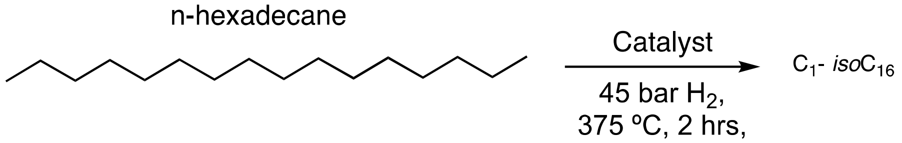


| Entry | Catalyst | Conv. (%) [g] | $C_{1\text{-}4}$ Yield (%) [g] | $C_{5\text{-}16}$ Yield (%) [g] | $H_2$ Cons. (%) [g] |
|---|---|---|---|---|---|
| 1 | Zeo-Y_H | 26.7±1.4 [0.42±0.02] | 3.3 [0.05] | 23.3 [0.37] | 11 [0.03] |
| 2 | Zeo-Y_H [60] | 24.6±1.2 [0.39±0.02] | 3.8 [0.06] | 20.8 [0.33] | 8 [0.02] |
| 3 | Zeo-Y_H [80] | 14.9±0.6 [0.24±0.01] | 2.0 [0.03] | 12.8 [0.20] | 6 [0.01] |
| 4 | Ni/Zeo-Y_H | 20.9±1.3 [0.33±0.02] | 0.4 [0.01] | 20.5 [0.31] | 8 [0.02] |
| 5 | Ni/Zeo-Y_H [60] | 5.8±0.5 [0.09±0.01] | 0.9 [0.01] | 4.9 [0.08] | 7 [0.02] |
| 6 | Ni/Zeo-Y_H [80] | 4.9±0.7 [0.08±0.01] | 0.6 [0.01] | 4.3 [0.07] | 4 [0.01] |
| 7 | Ru/Zeo-Y_H | 99.0±1.0 [1.57±0.02] | 92.4 [1.65] | 6.9 [0.11] | 85 [0.21] |
| 8 | Ru/Zeo-Y_H [60] | 99.0±1.0 [1.57±0.02] | 98.0 [1.76] | 2.0 [0.02] | 86 [0.21] |
| 9 | Ru/Zeo-Y_H [80] | 99.0±1.0 [1.57±0.02] | 97.2 [1.75] | 2.8 [0.03] | 87 [0.21] |

Reaction conditions: *n*-hexadecane (1.59 g, 7.0 mmol), catalyst (0.1 g, metal loading = 2.5 wt%), S/C ratio (substrate/catalyst weight ratio) ~16, 45 bar $H_2$, 375 ºC, 2 hrs. * All yields were calculated as the carbon yield and isomerized $C_{16}$ (*iso*$C_{16}$) are considered as products. Note that ~87% $H_2$ consumption (~105.0 mmol) is able to produce methane quantitatively due to the ~1.15 eq. $H_2$ stichometry.

**Supplementary Table 5** Degrees of saturation of the liquid products obtained from the deconstruction of *n*-hexadecane.

| Entry | Catalyst | Conversion (%) | Saturated (%, δ = 0.25-2.0) | Unsaturated (%, δ = 2.0-6.0) | Aromatic (%, δ = 6.0-8.0) |
|---|---|---|---|---|---|
| 1 | Zeo-Y_H | 26.7±1.4 | 98.8±0.1 | 1.2±0.1 | 0.1±0.1 |
| 2 | Zeo-Y_H [60] | 24.6±1.2 | 98.6±0.1 | 1.4±0.1 | 0.1±0.1 |
| 3 | Zeo-Y_H [80] | 14.9±0.6 | 98.7±0.1 | 1.3±0.1 | 0.1±0.1 |
| 4 | Ni/Zeo-Y_H | 20.9±1.3 | 99.8±0.2 | 0.2±0.2 | 0.1±0.1 |
| 5 | Ni/Zeo-Y_H [60] | 5.8±0.5 | 99.7±0.3 | 0.3±0.3 | 0.1±0.1 |
| 6 | Ni/Zeo-Y_H [80] | 4.9±0.7 | 99.5±0.5 | 0.5±0.5 | 0.1±0.1 |

Reaction conditions: *n*-hexadecane (1.59 g, 7.0 mmol), catalyst (0.1 g, metal loading = 2.5 wt%), 45 bar $H_2$, 375 ºC, 2 hrs. Note that degrees of saturation are defined by the ratio of proton integrations in the $^1$H NMR spectra to indicate the adjacent carbon-carbon bonds (saturated: δ = 0.25-2.0, unsaturated: δ = 2.0-6.0 and aromatics: δ = 2.0-6.0) given the C-H and C-C bond exclusivity of hydrocarbons.

**Supplementary References**


1. Biesinger, M. C. *et al.* Resolving surface chemical states in XPS analysis of first row transition metals, oxides and hydroxides: Cr, Mn, Fe, Co and Ni. *Appl. Surf. Sci.* **257**, 2717–2730 (2011).
2. Morgan, D. J. Resolving ruthenium: XPS studies of common ruthenium materials. *Surf. Interface Anal.* **47**, 1072–1079 (2015).